

Synthetic β -nitrostyrene derivative CYT-Rx20 as inhibitor of oral cancer cell proliferation and tumor growth through glutathione suppression and reactive oxygen species induction

Yen-Yun Wang, PhD,¹ Yuk-Kwan Chen, DDS, MS,^{2,3,4} Ya-Ling Hsu, MS,¹ Wen-Chin Chiu, PhD,⁵ Chun-Hao Tsai, MS,⁶ Stephen Chu-Sung Hu, MD, PhD,^{7,8} Pei-Wen Hsieh, PhD,^{9,10} Shyng-Shiou F. Yuan, MD, PhD^{1,6,11,12*}

¹Department of Medical Research, Kaohsiung Medical University Hospital, Kaohsiung Medical University, Kaohsiung, Taiwan, ²Division of Oral Pathology and Maxillofacial Radiology, Kaohsiung Medical University Hospital, Kaohsiung, Taiwan, ³School of Dentistry, College of Dental Medicine, Kaohsiung Medical University, Kaohsiung, Taiwan, ⁴Oral and Maxillofacial Imaging Center, College of Dental Medicine, Kaohsiung Medical University, Kaohsiung, Taiwan, ⁵Division of Thoracic Surgery, Department of Surgery, Kaohsiung Medical University Hospital, Kaohsiung Medical University, Kaohsiung, Taiwan, ⁶Graduate Institute of Medicine, College of Medicine, Kaohsiung Medical University, Kaohsiung, Taiwan, ⁷Department of Dermatology, Kaohsiung Medical University Hospital, Kaohsiung Medical University, Kaohsiung, Taiwan, ⁸Department of Dermatology, College of Medicine, Kaohsiung Medical University, Kaohsiung, Taiwan, ⁹Graduate Institute of Natural Products, School of Traditional Chinese Medicine, and Graduate Institute of Biomedical Sciences, College of Medicine, Chang Gung University, Taoyuan, Taiwan, ¹⁰Department of Anesthesiology, Chang Gung Memorial Hospital, Taoyuan, Taiwan, ¹¹Translational Research Center, Kaohsiung Medical University Hospital, Kaohsiung Medical University, Kaohsiung, Taiwan, ¹²Department of Obstetrics and Gynecology and Department of Medical Research, Kaohsiung Medical University Hospital, Kaohsiung Medical University, Kaohsiung, Taiwan.

Accepted 4 November 2016

Published online 27 March 2017 in Wiley Online Library (wileyonlinelibrary.com). DOI 10.1002/hed.24664

ABSTRACT: *Background.* The β -nitrostyrene family possesses anticancer properties. In this study, β -nitrostyrene derivative CYT-Rx20 (3'-hydroxy-4'-methoxy- β -methyl- β -nitrostyrene) was synthesized and investigated its anticancer activity in oral cancer.

Methods. Anticancer activity of CYT-Rx20 and the underlying mechanisms were analyzed using cell viability assay, reactive oxygen species (ROS) generation assay, fluorescence-activated cell sorter analysis, annexin V staining, comet assay, glutathione (GSH)/glutathione disulfide (GSSG) ratio, immunoblotting, soft agar assay, nude mice xenograft study, and immunohistochemistry.

Results. CYT-Rx20-induced cell apoptosis via ROS generation and mitochondrial membrane potential reduction, associated with release of mitochondrial cytochrome C to cytosol and activation of downstream

caspases and poly ADP-ribose polymerase (PARP). Furthermore, CYT-Rx20 induced mitochondrial ROS accumulation and mitochondrial dysfunction, followed by GSH downregulation. CYT-Rx20-induced cell apoptosis, ROS generation, and DNA damage were reversed by thiol antioxidants. In nude mice, CYT-Rx20 inhibited oral tumor growth accompanied by increased expression of γ H2AX, GSH reductase, and cleaved-caspase-3.

Conclusion. CYT-Rx20 has the potential to be further developed into an antitumor cancer drug clinically. © 2017 Wiley Periodicals, Inc. *Head Neck* 39: 1055–1064, 2017

KEY WORDS: β -Nitrostyrene, reactive oxygen species (ROS), glutathione (GSH), oral cancer, apoptosis

INTRODUCTION

Oral squamous cell carcinoma (OSCC) accounts for 3% of all newly diagnosed cancer cases and >90% of human oral malignancies, and ranks as the 11th most common cancer worldwide.^{1,2} Because of the high prevalence of betel-quid chewing in Taiwan, OSCC is the fourth most frequently occurring cancer and the fifth leading cause of cancer death in Taiwanese men.³ Despite substantial

advances in OSCC treatments, including surgery, radiotherapy, and chemotherapy, the prognosis for patients with advanced OSCC remains poor.⁴ The 5-year survival rate of early-stage (I and II) OSCC is approximately 80%, but that of advanced-stage (III and IV) OSCC is only around 20%.^{4,5} This highlights the need for continuous efforts to improve the treatment of patients with OSCC.

Platinum-based adjuvant treatment is currently one of the most commonly used chemotherapy regimens.⁶ However, its usefulness in OSCC could be constrained by the emergence of treatment resistance and side effects.⁷ Therefore, it is crucial to develop novel effective chemotherapy drugs with low toxicity for patients with OSCC.

The compounds in the β -nitrostyrene family inhibit protein tyrosine phosphatases⁸ and exert diverse biological functions, including antiplatelet and anticancer activities.^{9–11} β -nitrostyrene has been found to inhibit gastric cancer cell proliferation and immune responses of macrophages,¹² and

*Corresponding author: S.-S. F. Yuan, Translational Research Center, Kaohsiung Medical University Hospital, Kaohsiung Medical University, Kaohsiung, Taiwan. No.100, Tzyou 1st Road Kaohsiung 807, Taiwan. E-mail: yuanssf@ms33.hinet.net

Contract grant sponsor: This study was supported by grants from the Ministry of Health and Welfare (MOHW105-TDU-B-212-134007 and MOHW105-TDU-B-212-112016, Health and Welfare Surcharge of Tobacco Products) of Taiwan.

Additional Supporting Information may be found in the online version of this article.

its derivatives suppressed the tumor necrosis factor alpha/nuclear factor-kappa B signaling in a retinoid X receptor α -dependent manner to induce apoptosis in breast cancer cells.¹³

CYT-Rx20 (3'-hydroxy-4'-methoxy- β -methyl- β -nitrostyrene) has been found to impede platelet activity and induce breast cancer cell death.¹¹ In our previous work, we showed that CYT-Rx20 induced apoptosis in breast cancer cell death through reactive oxygen species (ROS)-mediated methyl ethyl ketone-extracellular signal-regulated kinase signaling.¹⁴ However, the chemotherapeutic consequence of CYT-Rx20 on OSCC, to our knowledge, has not been investigated. Therefore, the purpose of the current study was to explore the potential anticancer activities of CYT-Rx20 on OSCC and the underlying mechanisms.

MATERIALS AND METHODS

Reagents

CYT-Rx20 was synthesized, as previously described.¹⁵ Dulbecco modified Eagle's medium, dichlorofluorescein diacetate (DCFDA), and JC-1 were obtained from Invitrogen (Carlsbad, CA). Annexin V/PI apoptosis detection kit was obtained from BD Biosciences (Franklin Lakes, NJ). Fetal bovine serum, penicillin, streptomycin, and amphotericin B were obtained from Biological Industries (Beit Haemek, Israel). Propidium iodide, N-acetyl-L-cysteine (NAC), glutathione (GSH), and 2-mercaptoethanol (2-ME) were obtained from Sigma-Aldrich (St. Louis, MO). Mitochondrial ROS levels were assessed using MitoSOX Red (M36008; Invitrogen). Antibodies used in this study included cleaved-poly ADP-ribose polymerase (PARP) (#9541; Cell Signaling Technology, Danvers, MA), cleaved-caspase-3 (#9661S; Cell Signaling Technology), cleaved-caspase-7 (#9491; Cell Signaling Technology), histone H2AX (GTX80694; Genetex, Irvine, CA), β -actin (GTX110564; Genetex), and GSH reductase (GTX114199; Genetex). Other reagents used in the current study were indicated separately wherever suitable.

Cell culture

Human oral cancer cell lines (SAS, OCEM-1, and HSC-3) were included in this study. Cells were grown in Dulbecco modified Eagle's medium supplemented with 10% fetal bovine serum, 100 U/mL penicillin, 100 μ g/mL streptomycin, and 2.5 μ g/mL amphotericin B at 37°C in a 5% CO₂ incubator.

XTT cell viability assay

Cells from 3 human oral cancer cell lines (SAS, OCEM-1, and HSC-3) were seeded at 4×10^3 cells/well in 96-well plates and allowed to attach overnight. After treatment with CYT-Rx20 or cisplatin (CDDP) at various concentrations for 24 hours, cell viability was assessed by the XTT assay, according to a previous study.¹⁶

Immunoblotting analysis

The levels of caspase-associated proteins (caspase-3, caspase-7, and caspase-9), cleaved-PARP, and γ H2AX were analyzed by immunoblotting after treatment of cells

with CYT-Rx20 for 24 hours with the detailed procedures described in a previous report.¹⁷

Flow cytometry

Intracellular ROS content of human oral cancer cells was measured using H₂DCFDA fluorescent dye and determined by flow cytometry with the detailed procedures described in a previous report.¹⁸

Alkaline comet assay for detection of DNA single-strand breaks and double-strand breaks

Cells from 3 human oral cancer cell lines (SAS, OCEM-1, and HSC-3), after pretreatment with 5 mM NAC for 1 hour and cotreatment with 5 mM NAC and 1 μ g/mL CYT-Rx20 for 24 hours, were combined with 1% low melting point agarose at a ratio of 1:10 (v/v). Of the mixture, 75 μ l was immediately pipetted onto Comet Slide (Trevigen; Gaithersburg, MD) at 4°C and kept in the dark for 10 minutes. The slides were then immersed in prepared cold lysis solution (Trevigen) for 60 minutes. Subsequently, the slides were drained and placed in a horizontal gel electrophoresis apparatus containing freshly prepared alkaline buffer (300 mM NaOH, 1 mM EDTA, and pH >13) at 20 V for 30 minutes, and stained with 2.5 μ g/mL PI (Sigma-Aldrich) for 15 minutes. The mean tail moment was analyzed by CometScore software (TriTek; Sumerduck, VA).

Detection of mitochondrial reactive oxygen species and mitochondrial membrane potential

The levels of mitochondrial ROS and loss of mitochondrial membrane potential were determined by flow cytometry using MitoSOX Red and JC-1, respectively. Similar procedures were described in a previous study.¹⁸ Cells from 3 human oral cancer cell lines (SAS, OCEM-1, and HSC-3) were treated with 200 μ M H₂O₂ for 2 hours and mitochondrial O₂⁻ production was then measured by flow cytometry using the mitochondria-targeting O₂⁻ probe MitoSOX Red. JC-1 disaggregation representing the loss of mitochondrial membrane potential was determined after CYT-Rx20 treatment for 4 hours. Mean fluorescence intensity was determined by CellQuest software (BD Biosciences).

Mitochondrial isolation

Oral cancer cells, grown in 15-cm dishes and 4 hours after CYT-Rx20 treatment, were collected by trypsinization. Mitochondrial and cytosolic fractions from 2×10^7 cells per sample were isolated using the mitochondria isolation kit, in accord with the manufacturer's protocol (89874; Pierce, Rockford, IL) for determination of cytochrome C distribution.

Glutathione/glutathione disulfide assay

GSH/glutathione disulfide (GSSG) assay was applied to analyze the ratio of GSH to GSSG in the oral cancer cells lines (SAS, OCEM-1, and HSC-3). Cells were processed according to the instructions of the GSH and GSSG Assay Kit (K261-100; BioVision, Mountain View, CA), and GSH and GSSG levels were determined at Ex/Em

340/420 nm using a fluorescence microplate reader (FL×800; Biotek Instruments, Winooski, VT).

Anchorage-independent soft agar assay

Cells from 3 human oral cancer cell lines (SAS, OCEM-1, and HSC-3) were seeded at 1000 cells/well with 0.25% agar in 48-well plates, followed by treatment with CYT-Rx20 at the indicated concentrations for 24 hours. Cells were grown for 30 days and then stained with 0.5% crystal violet. Cell culture medium was changed every 2 to 3 days during the incubation period.

Ex vivo tumor xenograft study

The animal studies were approved by the Institutional Animal Care and Use Committee (no. 102009) of Kaohsiung Medical University, Taiwan. Animal experiments were approved by the Laboratory Animal Ethics Committee of the Kaohsiung Medical University and were conducted in accordance with the Animal Research: Reporting In Vivo Experiments guidelines. Six-week-old male immune-deficient BALB/cAnN.Cg-Foxn1^{nu}/CrlNarl mice from the National Laboratory Animal Center of Taiwan were subcutaneously injected with 3×10^6 SAS cells into both flanks. When the tumors grew to visible size (approximately an average diameter of 3 mm), the mice were intraperitoneally injected 3 times a week with 100 μ L normal saline-dissolved CYT-Rx20 at 1.0 μ g/g body weight or at 5.0 μ g/g body weight, whereas the control mice were injected with normal saline alone. Tumor volumes were calculated using the formula $\text{width}^2 \times \text{length}/2$. Tumor weights were measured when the mice were euthanized at the end of the experimental period.

Immunohistochemistry and hematoxylin-eosin staining

Immunohistochemical staining for γ H2AX, cleaved caspases-3, and GSH reductase were performed using the fully automated Bond-Max system and in accord with the manufacturer's instructions (Leica Microsystems, Wetzlar, Germany). For quantification, the staining of γ H2AX, cleaved caspases-3, and GSH reductase was calculated using the histochemical score, the product of percentage of stained cells, and intensity of staining.¹⁹ Besides, the tissues from various organs of mice were stained with hematoxylin-eosin.

Statistical analysis

Quantitative data were recorded as mean \pm SD or mean \pm SEM from 3 independent experiments. Differences between treatment groups were calculated by 1-way analyses of variance and post hoc Tukey's test for multiple comparisons. A *p* value $<$.05 was considered statistically significant.

RESULTS

CYT-Rx20 inhibited oral cancer cell viability through induction of apoptosis

To study the antioral cancer activity of CYT-Rx20, the cytotoxicity of CYT-Rx20 (Figure 1A) on 3 human oral cancer cell lines (SAS, OCEM-1, and HSC-3) was analyzed. The concentration of half inhibition of CYT-Rx20

on the 3 oral cancer cell lines was 0.92 ± 0.03 , 1.15 ± 0.03 , and 1.41 ± 0.05 μ g/mL, respectively. Notably, CYT-Rx20 had more potent cytotoxic activity than cisplatin in all 3 of the oral cancer cell lines that we examined (Figure 1B). CYT-Rx20 treatment increased the levels of cleaved caspases-9, 3, 7, cleaved PARP, and γ -H2AX (Figure 1C) in oral cancer cell lines, implying that caspase activation was involved in CYT-Rx20-induced oral cancer cell death. The CYT-Rx20-induced apoptotic cell death was further confirmed by Annexin V/PI staining results, which showed increased annexin V-positive cells after CYT-Rx20 treatment for 24 and 48 hours (Figure 1D).

Involvement of reactive oxygen species-mediated pathways in CYT-Rx20-induced cytotoxicity in oral cancer cells

ROS are crucial for signal transduction in response to environmental stress.^{20–22} The ROS levels in oral cancer cells, determined by flow cytometry using the H₂DCFDA fluorescent dye, were increased after CYT-Rx20 treatment (Figure 2A). Notably, the CYT-Rx20-induced ROS production was reversed by cotreatment with NAC, an ROS scavenger (Figure 2B). In addition, the CYT-Rx20-induced cell death was rescued in the presence of NAC (Figure 2C). The involvement of ROS in CYT-Rx20-reduced DNA damage was further determined, and the results showed that NAC significantly suppressed DNA double-strand breaks (Figure 2D) induced by CYT-Rx20 treatment in oral cancer cells.

CYT-Rx20-induced reactive oxygen species production-impaired mitochondrial function in oral cancer cells

Mitochondrial dysfunction, including aberrant ROS production and membrane potential, has been considered as a critical mechanism for apoptotic cell death.^{23,24} In this study, MitoSOX Red and JC-1 fluorescent probes were used to evaluate mitochondrial ROS production and membrane potential. Our data revealed that CYT-Rx20 treatment significantly enhanced mitochondrial ROS production, accompanied by loss of mitochondrial membrane potential ($\Delta\Psi$ m), as determined by JC-1 disaggregation (Figure 3A and 3B). We also examined the release of cytochrome C from mitochondria to cytosol by immunoblotting analysis, which showed that the cytosolic cytochrome C contents in oral cancer cells increased significantly after treatment with CYT-Rx20 for 4 hours (Figure 3C).

Reactive oxygen species-associated oral cancer cell death upon CYT-Rx20 treatment was rescued by thiol antioxidants

Because NAC was able to rescue oral cancer cell death induced by CYT-Rx20, we tested whether two other thiol antioxidants, GSH and 2-ME, had similar activity.^{25,26} Our results showed that CYT-Rx20-induced cytotoxicity was rescued in the presence of either GSH or 2-ME (Figure 4A). Furthermore, CYT-Rx20-induced ROS production was also reversed by GSH or 2-ME (Figure 4B).

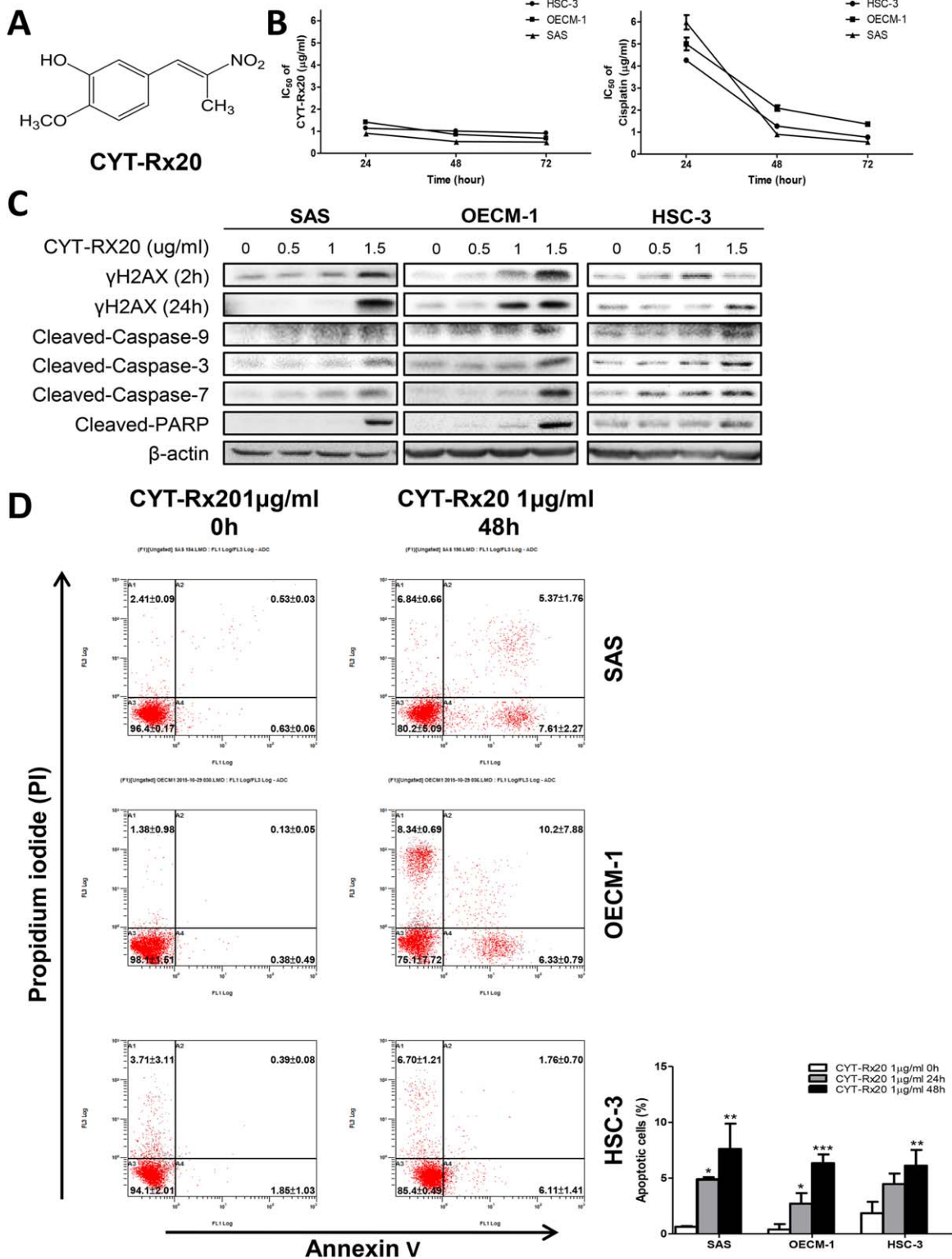
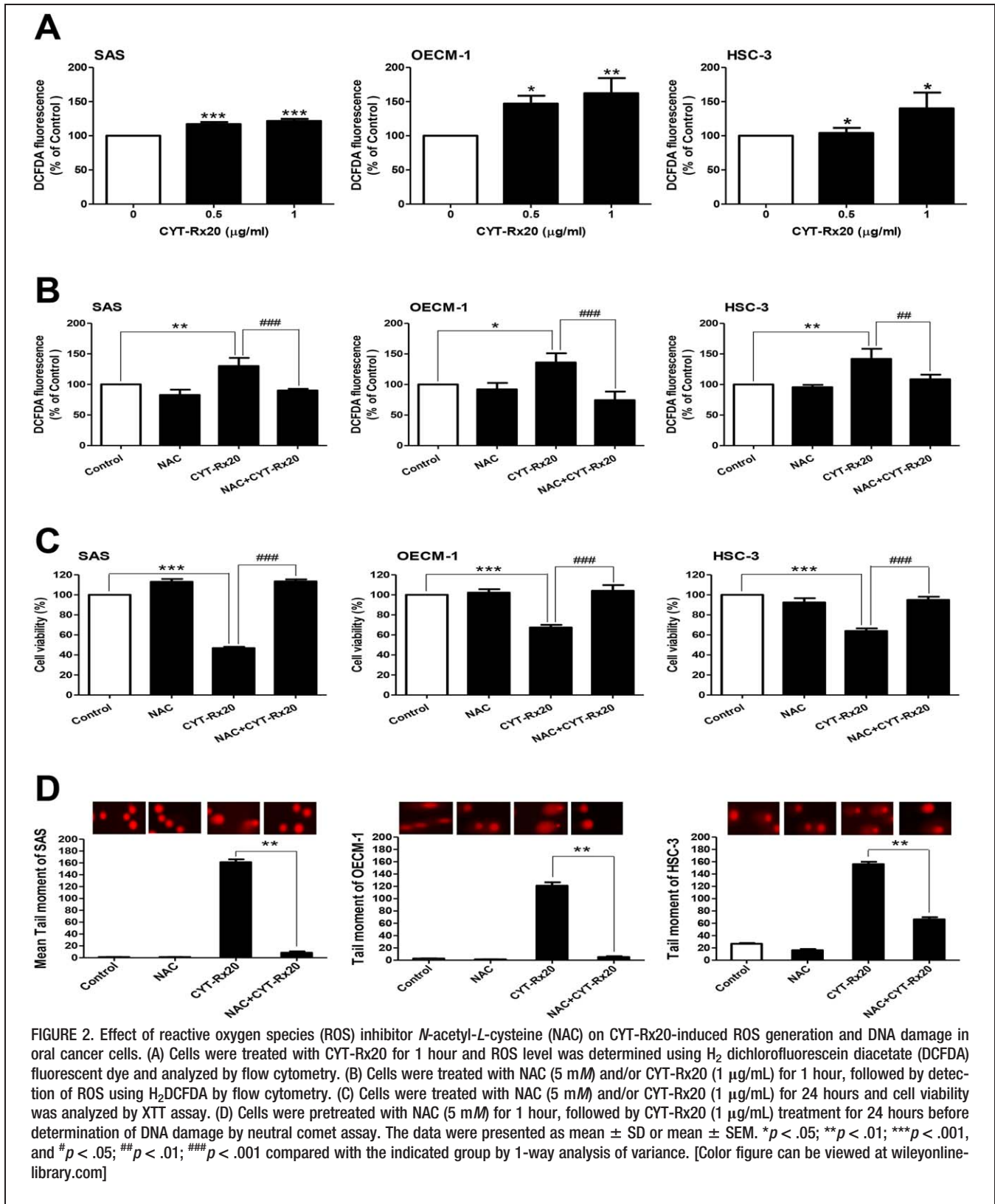


FIGURE 1. Cytotoxic effect of CYT-Rx20 on oral cancer cells. (A) Chemical structure of CYT-Rx20. (B) Effects of CYT-Rx20 and cisplatin (CDDP) on SAS, OECM-1, and HSC-3 cell viability. SAS, OECM-1, and HSC-3 cells were treated with various concentrations of CYT-Rx20 or CDDP for 24 hours and then cell viability was assessed by the XTT colorimetric assay. (C) The expression of apoptosis-related proteins in oral cancer cells treated with CYT-Rx20 for 24 hours were analyzed by immunoblotting. The expression of β-actin was used as the internal control. The results were representative of 3 separate experiments. (D) Oral cancer cell death after CYT-Rx20 (1 μg/mL) treatment for 24 hours was determined using Annexin V/PI staining followed by flow cytometric analysis. The data were presented as mean ± SD. **p* < .05; ***p* < .01; ****p* < .001 compared with the indicated group by 1-way analysis of variance. IC₅₀, concentration of half inhibition; PARP, poly ADP-ribose polymerase. [Color figure can be viewed at wileyonlinelibrary.com]



GSH deficiency leads to an increased susceptibility to oxidative stress and may, therefore, contribute to the progression of many disease states.^{27–29} In this study, we examined whether CYT-Rx20 altered intracellular GSH levels. Our data indicated that CYT-Rx20-treated oral

cancer cells not only showed reduced intracellular GSH levels but also showed a dose-dependent decrease of the GSH/GSSG ratio (Figure 4C).

GSH reductase is responsible for maintaining the supply of reduced GSH.³⁰ In this study, the effect of CYT-

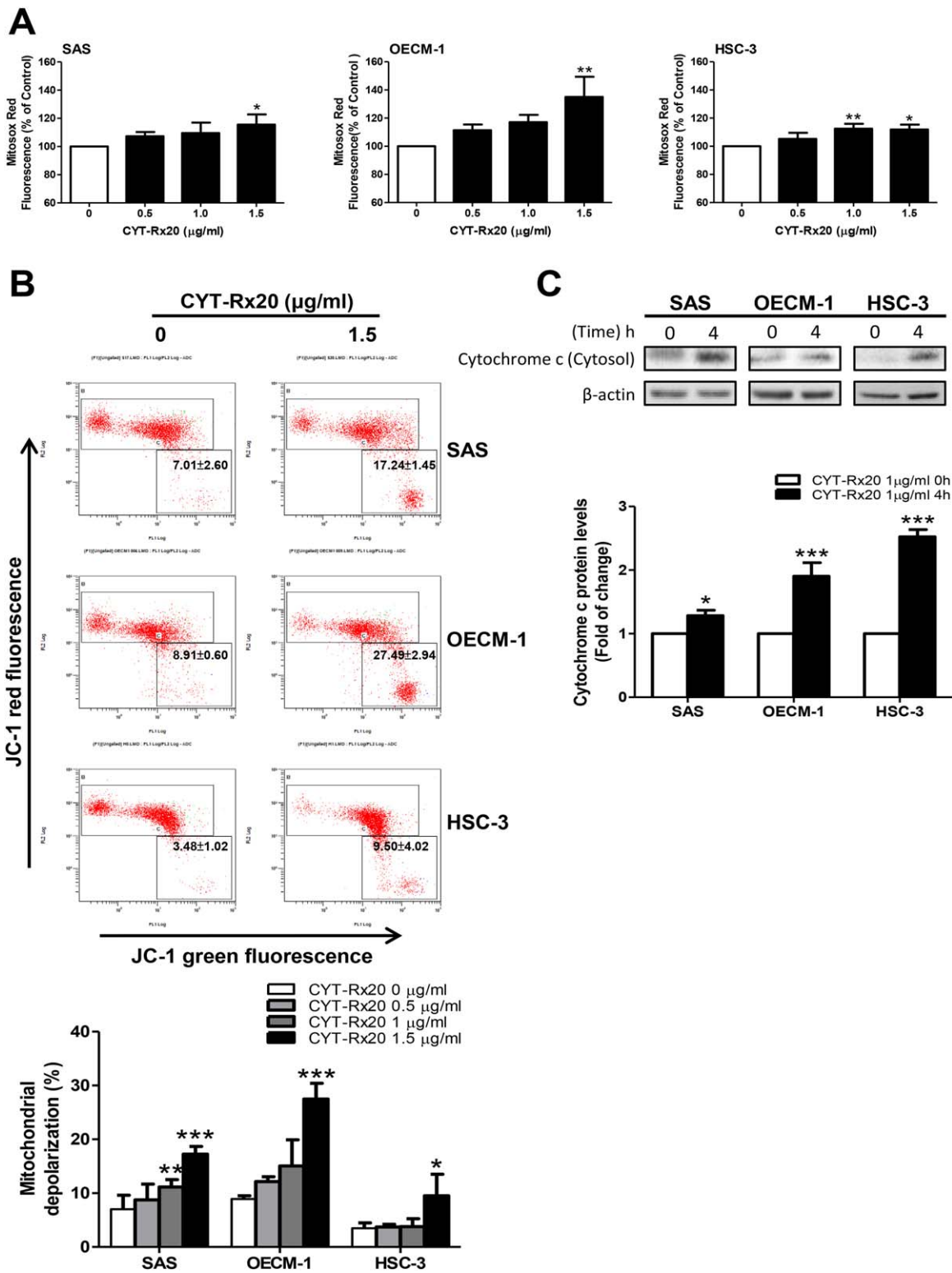


FIGURE 3. Effect of CYT-Rx20 on mitochondrial dysfunction in oral cancer cells. (A) Cells were treated with the indicated concentrations of CYT-Rx20 for 2 hours and mitochondrial O_2^- production was measured using the mitochondria-targeting O_2^- probe MitoSOX Red by flow cytometry. (B) Representative images of flow cytometry analysis showing changes in mitochondrial membrane potential. Cells were treated with the indicated concentrations of CYT-Rx20 for 4 hours and analyzed by flow cytometry. The green emission was analyzed in fluorescent channel 1 (FL 1; JC-1 green fluorescence) and the red emission in channel 2 (FL 2; JC-1 red fluorescence). (C) The expression levels of cytochrome C in the cytosolic fractions of oral cancer cell lines were analyzed by immunoblotting after CYT-Rx20 (1 μ g/mL) treatment. The expression of β -actin was used as the internal control. The data were presented as mean \pm SD. * $p < .05$; ** $p < .01$; *** $p < .001$ compared with the indicated group by 1-way analysis of variance. [Color figure can be viewed at wileyonlinelibrary.com]

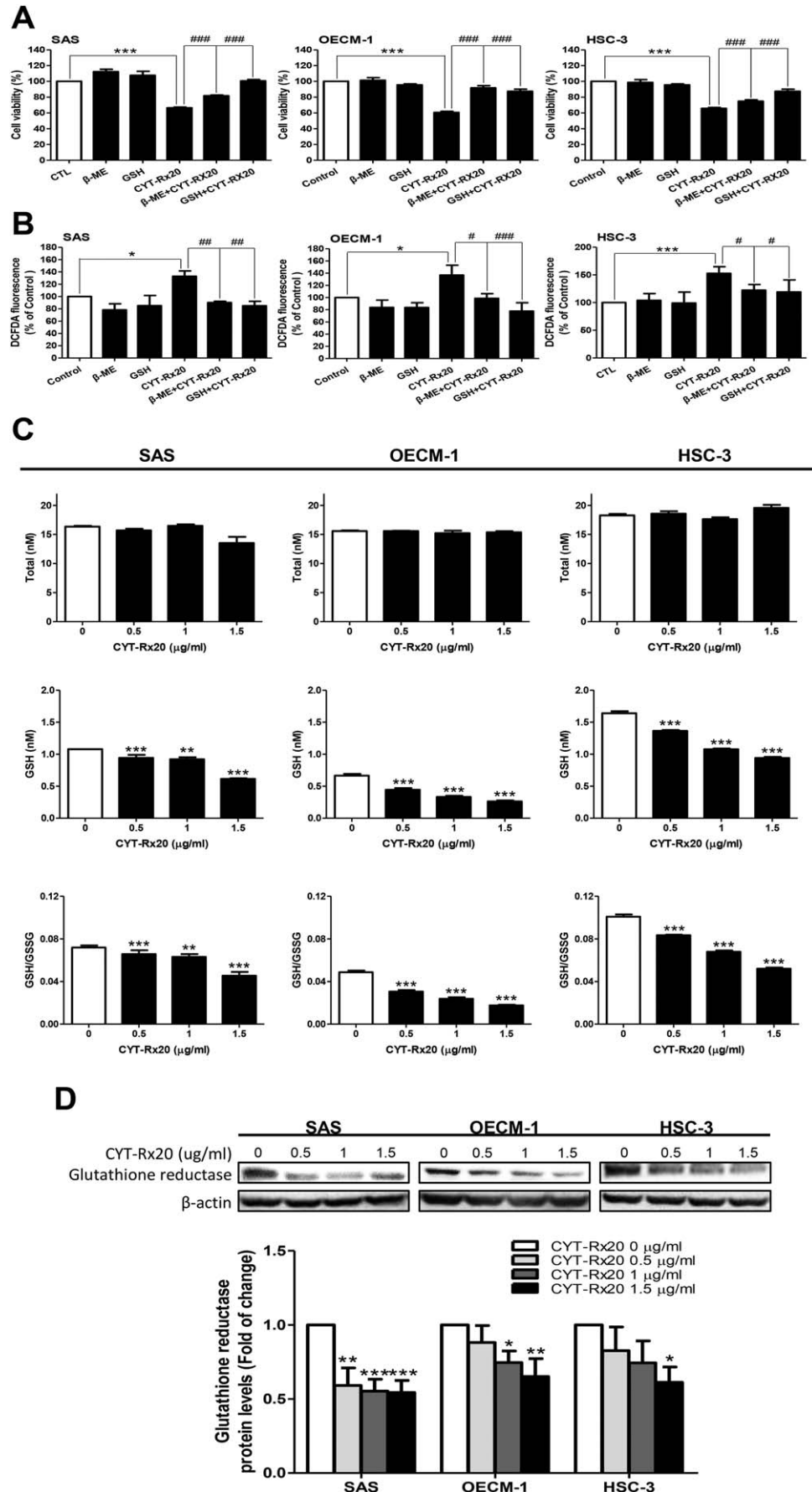


FIGURE 4. Effect of CYT-Rx20 on glutathione (GSH) level in oral cancer cells. (A) Cells were pretreated with GSH (1 mM) or 2-mercaptoethanol (2-ME; 100 μM) for 1 hour, followed by CYT-Rx20 (1.5 μg/mL) treatment for 24 hours before XTT assay. (B) Cells were treated with GSH (1 mM) or 2-ME (100 μM) and/or CYT-Rx20 (1 μg/mL) for 1 hour and reactive oxygen species (ROS) level was determined by flow cytometry. (C) Oral cancer cells were incubated with the indicated concentrations of CYT-Rx20 for 2 hours and then cellular GSH levels and GSH/glutathione disulfide (GSSG) ratios were determined. (D) The expression levels of GSH reductase in oral cancer cells were analyzed by immunoblotting after CYT-Rx20 treatment for 2 hours. The expression of β-actin was used as the internal control. The data were presented as mean ± SD. **p* < .05; ***p* < .01; ****p* < .001; and #*p* < .05; ##*p* < .01; ###*p* < .001 compared with the indicated group by 1-way analysis of variance. DCFDA, dichlorofluorescein diacetate.

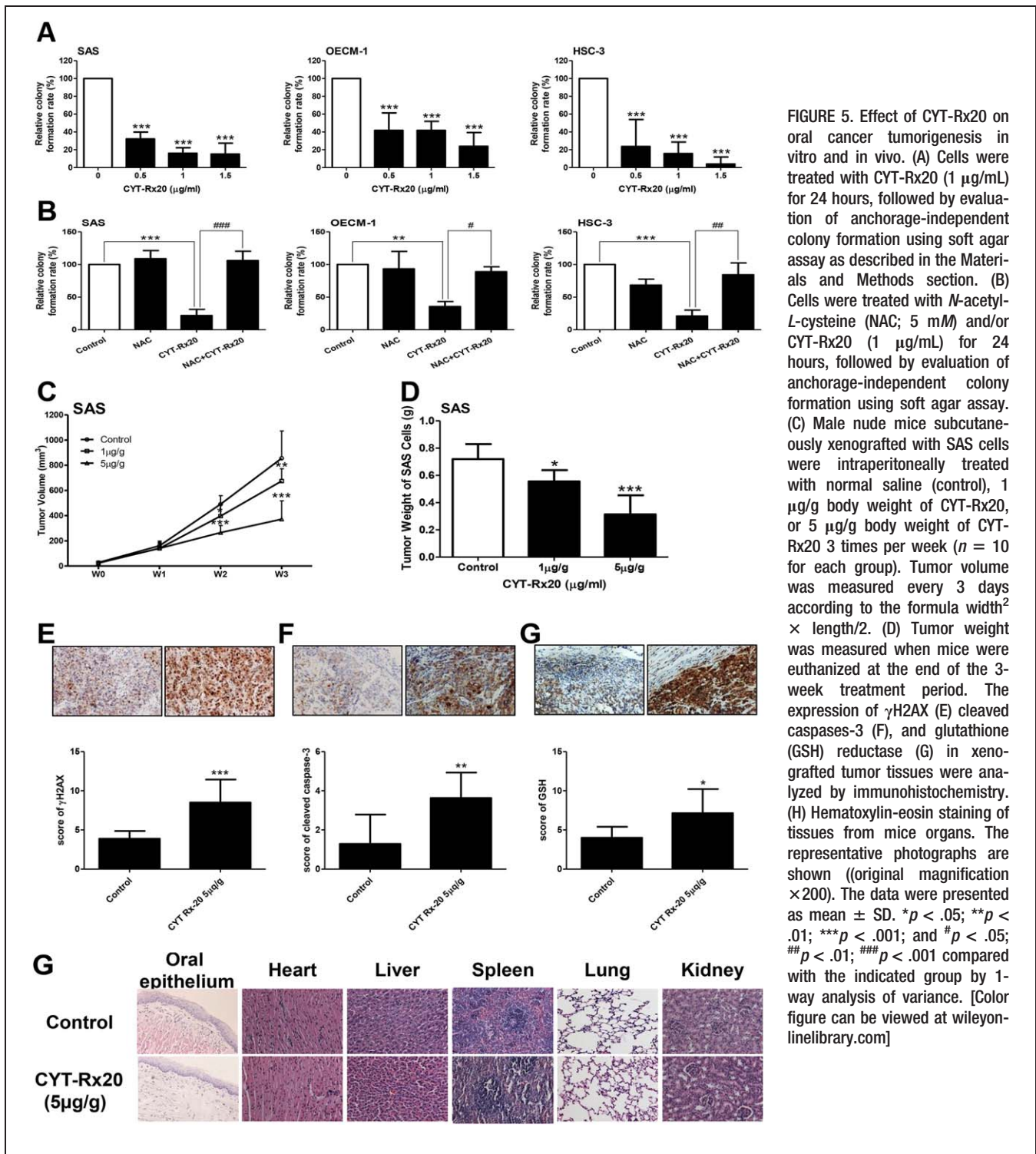


FIGURE 5. Effect of CYT-Rx20 on oral cancer tumorigenesis in vitro and in vivo. (A) Cells were treated with CYT-Rx20 (1 μg/mL) for 24 hours, followed by evaluation of anchorage-independent colony formation using soft agar assay as described in the Materials and Methods section. (B) Cells were treated with *N*-acetyl-L-cysteine (NAC; 5 mM) and/or CYT-Rx20 (1 μg/mL) for 24 hours, followed by evaluation of anchorage-independent colony formation using soft agar assay. (C) Male nude mice subcutaneously xenografted with SAS cells were intraperitoneally treated with normal saline (control), 1 μg/g body weight of CYT-Rx20, or 5 μg/g body weight of CYT-Rx20 3 times per week ($n = 10$ for each group). Tumor volume was measured every 3 days according to the formula $\text{width}^2 \times \text{length} / 2$. (D) Tumor weight was measured when mice were euthanized at the end of the 3-week treatment period. The expression of γ H2AX (E) cleaved caspases-3 (F), and glutathione (GSH) reductase (G) in xenografted tumor tissues were analyzed by immunohistochemistry. (H) Hematoxylin-eosin staining of tissues from mice organs. The representative photographs are shown (original magnification $\times 200$). The data were presented as mean \pm SD. * $p < .05$; ** $p < .01$; *** $p < .001$; and # $p < .05$; ## $p < .01$; ### $p < .001$ compared with the indicated group by 1-way analysis of variance. [Color figure can be viewed at wileyonlinelibrary.com]

Rx20 on the protein expression of GSH reductase was examined. We found that CYT-Rx20 treatment decreased GSH reductase levels in oral cancer cells in a dose-dependent manner (Figure 4D).

CYT-Rx20 inhibited xenografted tumor growth in mice

The inhibitory effect of CYT-Rx20 on in vitro anchorage-independent growth of oral cancer cells was

evaluated by soft agar assay. The results showed that CYT-Rx20 inhibited significantly the anchorage-independent growth of oral cancer cells (Figure 5A), and the CYT-Rx20-induced growth inhibition was rescued by NAC (Figure 5B). To further explore the anticancer activity of CYT-Rx20 in vivo, a nude mice xenograft tumor growth model was used. As shown in Figure 5C and 5D, CYT-Rx20 significantly suppressed xenografted tumor growth. After CYT-Rx20 treatment for 3 weeks, the

average tumor volumes for the control, CYT-Rx20 (1.0 $\mu\text{g/g}$ body weight), and CYT-Rx20 (5.0 $\mu\text{g/g}$ body weight) groups were 855.43 ± 217.49 , 674.43 ± 98.41 , and $372.27 \pm 145.56 \text{ mm}^3$, respectively (Figure 5C), whereas the average tumor weights at euthanasia were 0.72 ± 0.11 , 0.56 ± 0.08 , and $0.31 \pm 0.14 \text{ g}$, respectively (Figure 5D). Furthermore, the expressions of γH2AX (Figure 5E), GSH reductase (Figure 5F), and cleaved caspases-3 (Figure 5G) in xenografted tumors were increased in mice treated with CYT-Rx20, consistent with our in vitro observation. No significant differences were observed in the body weight (Appendix Figure S3, online only), blood biochemical parameters (Appendix Table S1, online only), and histology of the oral epithelium, heart, liver, spleen, lungs, and kidneys between CYT-Rx20-treated mice and control mice (Figure 5H).

DISCUSSION

In the current study, we demonstrated, we believe for the first time, that CYT-Rx20, a synthetic derivative of β -nitrostyrene, significantly reduced cell viability and induced apoptotic cell death in oral cancer cells, and it exhibited a higher potency against oral cancer cells than the clinically used chemotherapeutic agent CDDP. CYT-Rx20 also decreased oral tumor growth in an in vivo mouse xenograft model. These results provide in vitro and in vivo evidence for the antineoplastic activity of CYT-Rx20 in oral cancer.

ROS are produced as a normal product of cellular metabolism. Various environmental stresses lead to excessive production of ROS, causing progressive oxidative damage and ultimately cell death. Under the conditions of environmental stress, ROS can be overproduced and then interfere with the stability of mitochondrial membrane potential, leading to an excessive amount of mitochondria-mediated release of ROS, which further promotes cell death.³¹ Previous studies suggested that CDDP not only induced DNA damage but also induced ROS production, which triggers cell death.³² In the present study, we provided evidence that ROS was critically involved in the anticancer effects of CYT-Rx20 on oral cancer cells. Furthermore, ROS can be generated through uncontrolled electron delivery or deficiency in ROS scavengers, such as GSH, a major intracellular antioxidant known to be involved in ROS elimination.^{33,34} In this study, we found that the CYT-Rx20-induced cytotoxicity in oral cancer cells was significantly restored by thiol antioxidants, such as NAC, GSH, and β -mercaptoethanol, suggesting that the anticancer activities of CYT-Rx20 may result from the imbalance of thiol redox status.

GSH reductase is an essential enzyme that recycles oxidized GSH back to the reduced form and the reduced form of GSH can scavenge reactive oxygen and nitrogen species, thereby contributing to the control of redox homeostasis.³⁰ The results from the current study showed a significant decrease of GSH levels and GSH/GSSG ratios in oral cancer cells after CYT-Rx20 treatment. The levels of GSH reductase were also noted to be decreased in oral cancer cells treated with CYT-Rx20. Taken together, our study suggested that the failure of the antioxidant system to neutralize ROS may contribute to

excessive ROS accumulation and ultimately leads to cell death.

Induction of apoptosis is recognized as a major anticancer mechanism for many chemotherapeutic agents, including the currently studied CYT-Rx20.¹⁰ Previous studies reported that the caspase family mediated apoptotic programmed cell death in oral cancer.^{35,36} Caspase-9 is activated very early in the apoptotic cascade by cytochrome C, which is released from the mitochondria in response to apoptotic stimuli, and then downstream caspases, such as caspase-3, are activated leading to the cleavage of key cellular proteins, such as PARP. In this study, treatment of oral cancer cells with CYT-Rx20 resulted in the activation of caspase-9, caspase-3, caspase-7, and the cleavage of PARP, in agreement with the aforementioned reports.

Previous studies have also reported that mitochondrial dysfunction may cause the collapse of mitochondria membrane potential and result in mitochondrial permeability transition pore opening, leading to the release of cytochrome C from mitochondria into cytosol.²⁴ In this study, mitochondrially located ROS was detected rapidly after CYT-Rx20 treatment. In addition, a rapid increase in mitochondrial transmembrane potential ($\Delta\Psi\text{m}$) was detected and led to the release of cytochrome C from the mitochondria and the activation of caspases in oral cancer cells. Collectively, our data demonstrated that mitochondria-regulated apoptosis was involved in CYT-Rx20-induced oral cancer cell death.

The anticancer activity of CYT-Rx20 was also evaluated in vivo in our study. We found that CYT-Rx20 suppressed xenografted oral tumor growth associated with the increased expression of $\gamma\text{-H2AX}$, cleaved PARP, and cleaved-caspases-3 in tumor tissues. There were no obvious abnormal histological changes in major organs of nude mice (especially oral epithelium), and no impairment in hematopoiesis, renal, or liver function (Appendix Table S1, online only), rendering CYT-Rx20 a potential antitumor agent with low toxicity. On the other hand, CYT-Rx20 treatment of oral cancer cells inhibited cell migration and invasion in a dose-dependent manner (Appendix Figure S2, online only), suggesting that CYT-Rx20 inhibited not only the proliferation but also the metastasis of oral cancer cells.

In conclusion, the present study demonstrated that the synthetic β -nitrostyrene derivative CYT-Rx20 induced apoptosis in oral cancer cells through GSH downregulation and ROS induction with the detailed molecular mechanisms illustrated in Appendix Figure S4, online only. Our findings indicate that CYT-Rx20 may be developed as a potential chemotherapeutic agent for oral cancer. Further preclinical and clinical studies are required to confirm its therapeutic potential for oral cancer.

REFERENCES

- Rivera C, Venegas B. Histological and molecular aspects of oral squamous cell carcinoma (review). *Oncol Lett* 2014;8:7–11.
- Markopoulos AK. Current aspects on oral squamous cell carcinoma. *Open Dent J* 2012;6:126–130.
- Wang YY, Tail YH, Wang WC, et al. Malignant transformation in 5071 southern Taiwanese patients with potentially malignant oral mucosal disorders. *BMC Oral Health* 2014;14:99.
- Scott SE, Grunfeld EA, McGurk M. The idiosyncratic relationship between diagnostic delay and stage of oral squamous cell carcinoma. *Oral Oncol* 2005;41:396–403.

5. Brocklehurst P, Kujan O, O'Malley LA, Ogden G, Shepherd S, Glenn AM. Screening programmes for the early detection and prevention of oral cancer. *Cochrane Database Syst Rev* 2013;11:CD004150.
6. Florea AM, Busselberg D. Cisplatin as an anti-tumor drug: cellular mechanisms of activity, drug resistance and induced side effects. *Cancers (Basel)* 2011;3:1351–1371.
7. Stordal B, Davey M. Understanding cisplatin resistance using cellular models. *IUBMB Life* 2007;59:696–699.
8. Park J, Pei D. Trans-beta-nitrostyrene derivatives as slow-binding inhibitors of protein tyrosine phosphatases. *Biochemistry* 2004;43:15014–15021.
9. Chen IH, Chang FR, Wu YC, Kung PH, Wu CC. 3,4-Methylenedioxy- β -nitrostyrene inhibits adhesion and migration of human triple-negative breast cancer cells by suppressing β 1 integrin function and surface protein disulfide isomerase. *Biochimie* 2015;110:81–92.
10. Rahmani-Nezhad S, Safavi M, Pordeli M, et al. Synthesis, in vitro cytotoxicity and apoptosis inducing study of 2-aryl-3-nitro-2H-chromene derivatives as potent anti-breast cancer agents. *Eur J Med Chem* 2014;86:562–569.
11. Hsieh PW, Chang YT, Chuang WY, Shih HC, Chiang SZ, Wu CC. The synthesis and biologic evaluation of anti-platelet and cytotoxic β -nitrostyrenes. *Bioorg Med Chem* 2010;18:7621–7627.
12. Carter KC, Finnon YS, Daeid NN, Robson DC, Waddell R. The effect of nitrostyrene on cell proliferation and macrophage immune responses. *Immunopharmacol Immunotoxicol* 2002;24:187–197.
13. Zeng Z, Sun Z, Huang M, et al. Nitrostyrene derivatives act as RXR α ligands to inhibit TNF α activation of NF- κ B. *Cancer Res* 2015;75:2049–2060.
14. Hung AC, Tsai CH, Hou MF, et al. The synthetic β -nitrostyrene derivative CYT-Rx20 induces breast cancer cell death and autophagy via ROS-mediated MEK/ERK pathway. *Cancer Lett* 2016;371:251–261.
15. Wang WY, Hsieh PW, Wu YC, Wu CC. Synthesis and pharmacological evaluation of novel beta-nitrostyrene derivatives as tyrosine kinase inhibitors with potent antiplatelet activity. *Biochem Pharmacol* 2007;74:601–611.
16. Chen YJ, Chen HP, Cheng YJ, et al. The synthetic flavonoid WYC02-9 inhibits colorectal cancer cell growth through ROS-mediated activation of MAPK14 pathway. *Life Sci* 2013;92:1081–1092.
17. Chen YJ, Cheng YJ, Hung AC, et al. The synthetic flavonoid WYC02-9 inhibits cervical cancer cell migration/invasion and angiogenesis via MAPK14 signaling. *Gynecol Oncol* 2013;131:734–743.
18. Chen HM, Wu YC, Chia YC, et al. Gallic acid, a major component of *Toona sinensis* leaf extracts, contains a ROS-mediated anti-cancer activity in human prostate cancer cells. *Cancer Lett* 2009;286:161–171.
19. Sarbia M, Stahl M, Fink U, Willers R, Seeber S, Gabbert HE. Expression of apoptosis-regulating proteins and outcome of esophageal cancer patients treated by combined therapy modalities. *Clin Cancer Res* 1998;4:2991–2997.
20. Alfadda AA, Sallam RM. Reactive oxygen species in health and disease. *J Biomed Biotechnol* 2012;2012:936486.
21. Costa A, Scholer-Dahirel A, Mechta-Grigoriou F. The role of reactive oxygen species and metabolism on cancer cells and their microenvironment. *Semin Cancer Biol* 2014;25:23–32.
22. Reczek CR, Chandel NS. ROS-dependent signal transduction. *Curr Opin Cell Biol* 2015;33:8–13.
23. Sena LA, Chandel NS. Physiological roles of mitochondrial reactive oxygen species. *Mol Cell* 2012;48:158–167.
24. Pieczenik SR, Neustadt J. Mitochondrial dysfunction and molecular pathways of disease. *Exp Mol Pathol* 2007;83(1):84–92.
25. Rushworth GF, Megson IL. Existing and potential therapeutic uses for N-acetylcysteine: the need for conversion to intracellular glutathione for antioxidant benefits. *Pharmacol Ther* 2014;141:150–159.
26. Wong S, Kirkland JL, Schwanz HA, et al. Effects of thiol antioxidant β -mercaptoethanol on diet-induced obese mice. *Life Sci* 2014;107:32–41.
27. Traverso N, Ricciarelli R, Nitti M, et al. Role of glutathione in cancer progression and chemoresistance. *Oxid Med Cell Longev* 2013;2013:972913.
28. Aquilano K, Baldelli S, Ciriolo MR. Glutathione: new roles in redox signaling for an old antioxidant. *Front Pharmacol* 2014;5:196.
29. Balendiran GK, Dabur R, Fraser D. The role of glutathione in cancer. *Cell Biochem Funct* 2004;22:343–352.
30. Couto N, Wood J, Barber J. The role of glutathione reductase and related enzymes on cellular redox homeostasis network. *Free Radic Biol Med* 2016;95:27–42.
31. Dickinson BC, Chang CJ. Chemistry and biology of reactive oxygen species in signaling or stress responses. *Nat Chem Biol* 2011;7:504–511.
32. Brozovic A, Ambriovic-Ristov A, Osmak M. The relationship between cisplatin-induced reactive oxygen species, glutathione, and BCL-2 and resistance to cisplatin. *Crit Rev Toxicol* 2010;40:347–359.
33. Pan ST, Qin Y, Zhou ZW, et al. Plumbagin induces G2/M arrest, apoptosis, and autophagy via p38 MAPK- and PI3K/Akt/mTOR-mediated pathways in human tongue squamous cell carcinoma cells. *Drug Des Devel Ther* 2015;9:1601–1626.
34. Armstrong JS, Steinauer KK, Hornung B, et al. Role of glutathione depletion and reactive oxygen species generation in apoptotic signaling in a human B lymphoma cell line. *Cell Death Differ* 2002;9:252–263.
35. Loro LL, Vinternyr OK, Johannessen AC. Cell death regulation in oral squamous cell carcinoma: methodological considerations and clinical significance. *J Oral Pathol Med* 2003;32:125–138.
36. Karthikeyan S, Laxmanappa Hoti S, Nazeer Y, Vasudev Hegde H. Glaucaurbinone sensitizes KB cells to paclitaxel by inhibiting ABC transporters via ROS-dependent and p53-mediated activation of apoptotic signaling pathways. *Oncotarget* 2016;7:42353–42373.